Growth and photoluminescence of GaSb and $Ga_{1-x}In_xAs_ySb_{1-y}$ grown on GaSb substrates by liquid-phase electroepitaxy

S. Iyer
Department of Electrical Engineering, North Carolina A&T State University, Greensboro, North Carolina 27411

S. Hegde
University of Dayton Research Institute, Dayton, Ohio 45469-0178

Ali Abul-Fadl
Department of Electrical Engineering, North Carolina A&T State University, Greensboro, North Carolina 27411

K. K. Bajaj
Department of Physics, Emory University, Atlanta, Georgia 30322

W. Mitchel
Materials Directorate, Wright Laboratory, Wright–Patterson Air Force Base, Dayton, Ohio 45433-6533
(Received 5 February 1992; revised manuscript received 13 August 1992)

We report on the liquid-phase electroepitaxial (LPEE) growth of GaSb and $Ga_{1-x}In_xAs_ySb_{1-y}$ alloys on undoped (100) GaSb substrates. Alloys with room-temperature photoluminescence peak wavelengths as long as 2.32 μm have been grown. These layers were assessed by x-ray diffraction, energy-dispersive x-ray analysis, and low-temperature Fourier-transform photoluminescence (PL), with emphasis on the latter. The variation in the low-temperature photoluminescence bands as a function of the alloy composition has been investigated. The low-temperature (4.5 K) PL spectra of the alloys exhibited narrow peaks with full width half maxima in the range 3–7 meV, indicating an excellent quality of the LPEE-grown epilayers. The temperature and intensity dependences of the PL spectra were investigated to identify the nature of the recombination processes.

I. INTRODUCTION

The quaternary alloys $Ga_{1-x}In_xAs_ySb_{1-y}$ are currently of great interest for use in infrared devices (1.7–4.1 μm). The unique feature of this alloy system is the presence of the miscibility gap which covers almost the entire composition range at typical growth temperatures (Fig. 1). Nonequilibrium techniques, namely, organometallic vapor-phase epitaxy[1,2] (OMVPE) and molecular-beam epitaxy,[3,4] (MBE), have been used successfully for the growth of these layers in the miscibility gap region. The layers grown by liquid phase epitaxy[5–10] (LPE) are limited by the presence of the miscibility gap, and the composition with the longest wavelength reported inside the gap is 2.33 μm,[5] corresponding to x of 0.22 and 0.18 on GaSb substrates. For compositions away from the substrate corresponding to $x \geq 0.8$ (Refs. 8 and 9) difficulties have been encountered due to the growth solutions tending to dissolve the substrate. Hence, most of the LPE work has been concentrated over a very narrow composition range, for $x < 0.25$ (Refs. 5–7) on GaSb substrates and for $x \leq 0.2$ (Refs. 7 and 8) and $x \geq 0.83$ (Refs. 8 and 10) on InAs substrates.

Iyer *et al.*[11] have reported the growth of these layers lattice matched to GaSb by the liquid phase electroepitaxial (LPEE) technique. In the LPEE technique, unlike LPE, growth is carried out at a constant furnace temperature and is induced and sustained by an external parameter, in this case the current density. The advantages of LPEE over LPE-grown layers in terms of the interface stability,[12] surface morphology[13] and the compositional homogeneity[14,15] are well established. Epitaxial layers of InSb (Ref. 16) were the first binary III-V semiconductor compound layers grown by this technique. However, since then GaAs,[13] InSb,[16] InP,[17] GaP,[18] InAs,[19] $Ga_{1-x}Al_xAs$,[15] $In_{1-x}Ga_xAs$,[20,21] InGaP,[14] and $Ga_{1-x}In_xAs_yP_{1-y}$ (Ref. 22) have been grown by this technique.

GaSb, unlike other commonly known III-V semiconductors such as GaAs and InP, has a somewhat large concentration of residual acceptors. The dominant residual acceptor has been attributed to the native defect caused by Sb deficiency, predominantly due to either the Ga antisite,[23] or a Ga antisite in the vicinity of a Ga vacancy.[24–26] The nature of this acceptor has been a subject of extensive studies to determine whether the residual acceptor is a single acceptor[24,27] or a double acceptor.[28,30] The strong evidence of the latter has been shown in compensated materials,[28,29] namely, in donor-doped layers. The first and second ionization energy levels of this acceptor have been determined to be in the range 30–35 meV (Refs. 23, 28, and 29) and 70–120 meV (Refs. 28–30), respectively. In addition, another dominant acceptor level is present at 54 meV above the valence band

in GaSb.[27,31] However, the nature of this acceptor level is not well understood. Very little is known about the acceptors due to chemical impurities in this material.

The low-temperature photoluminescence has so far been an important characterization tool for assessing the quality of GaSb layers. Due to the presence of different acceptor levels in this material, the low-temperature PL spectra exhibit numerous transitions which include free excitons, recombinations at the different acceptor levels, and excitons bound to these neutral acceptor levels. Hence, if the layers grown are not of high purity, there is considerable misinterpretation of the origin of the PL peaks. The sharp structures near the band edge in GaSb have been attributed to excitons bound to different neutral acceptors.[27,32,33] In high-quality GaSb material, four bound excitons have been resolved[32,33] at low temperatures occurring at 805.4, 803.4, 800.1, and 796.1 meV, respectively. They will be referred to as BE_1, BE_2, BE_3, and BE_4, respectively, following the nomenclature of Ruhle and Bimberg,[32] which is now commonly used. The binding energies of excitons to the acceptors are significantly different and much larger than commonly observed in other III-V semiconductors such as GaAs, InP, and InSb. Both Johnson and Fan[30] and Benoit a la Guillaume and Lavallard[27] have identified BE_2 to correspond to an exciton bound to a native acceptor level at 34 meV, from Zeeman splitting and piezoemission experiments, respectively. The BE_4 transition has also been ascribed to an exciton bound to a neutral acceptor level[27,32] above the valence band from the piezoemission data.[27] However, Johnson and Fan[30] have suggested the possibility of this transition being due to an exciton bound to an ionized acceptor, while Pollak and Aggarwal[34] claimed to observe no splitting of the levels under uniaxial stress questioning the identity of the above transitions. The origin of the other two bound exciton transitions BE_1 and BE_3 is not yet clearly understood.

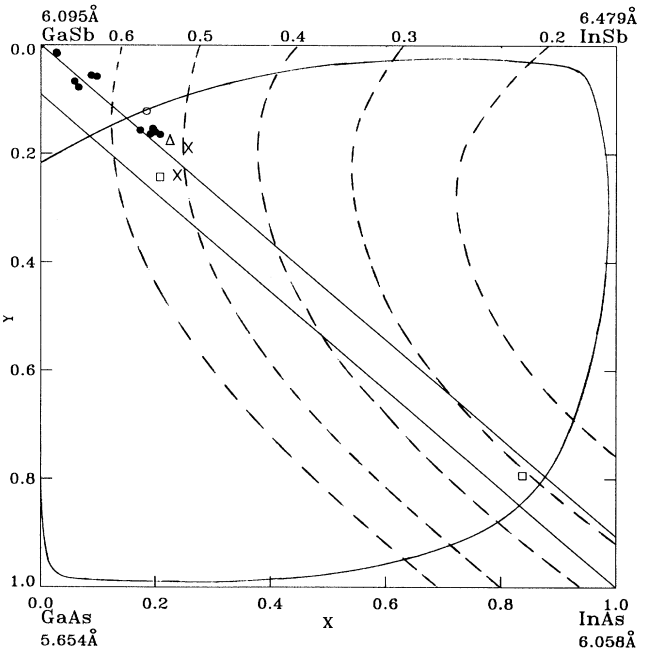

FIG. 1. Schematic diagram of the solid phase field for the quaternary alloy system $Ga_{1-x}In_xAs_ySb_{1-y}$. Isolattice constant lines for alloys lattice matched to GaSb and InAs are shown by the solid straight lines. Binodal isotherm at 600 °C and room-temperature band-gap plots are taken from Ref. 1. Indicated are our data points (●), previous LPE data corresponding to the highest value of x inside the gap lattice matched to GaSb, DeWinter *et al.* (Ref. 5) (Δ), Jouille *et al.* (Ref. 6) (×), and lattice matched to InAs, Sankaran and Antypas (Ref. 8) (□) and Astles *et al.* (Ref. 7) (○).

While there have been several reports on GaSb, there has been no detailed study of the radiative transitions in $Ga_{1-x}In_xAs_ySb_{1-y}$. As is well known for III-V semiconductor compounds and alloys in general, the properties of the material are growth specific. Hence, it becomes important to compare specific fundamental characteristics and the quality of the materials grown by LPEE technique with those grown using other techniques, in particular the LPE technique. In this work, we present a systematic study of the LPEE-grown $Ga_{1-x}In_xAs_ySb_{1-y}$ layers of compositions corresponding to the room-temperature wavelength in the range 1.7–2.28 μm. The results of the dependence of PL characteristics on the excitation laser power, temperature, and the alloy composition are reported.

II. EXPERIMENTAL DETAILS

A conventional horizontal slider boat system which was designed to allow the passage of current through the melt-substrate interface, was used for the LPEE growth of $Ga_{1-x}In_xAs_ySb_{1-y}$. The details of the growth system and the growth procedure have been described elsewhere.[11,20] Undoped (100) GaSb wafers of thickness 0.4 mm (16 mil) and an area of 6 mm × 6 mm were used as substrates. GaSb and three different compositions of the quaternary alloys were grown. The liquidus composition of the melt was determined by the source dissolution technique. Excess GaSb was added prior to epilayer growth to provide a continuous source of Sb. The lattice mismatch of the layers were determined either by double-crystal x-ray diffraction or by high-resolution x-ray diffraction. The rocking curves were recorded for the (400) reflection of Cu $K\alpha$ line from an InP and Si monochromator crystals, respectively.

The low-temperature PL spectra were obtained using a BOMEM Fourier-transform spectrometer at a resolution of 0.2 meV. An Ar-ion laser operating at 514.5 nm provided the excitation source. The maximum output power was limited to 140 mW. The spectra were taken using a focused laser spot on the sample and a liquid-nitrogen-cooled InAs as the detector. The beam diameter on the sample was 100–500 μm and typical excitation power density on the sample was ~ 1 W/cm^2. The low-temperature measurements were carried out in a variable temperature continuous-flow liquid-helium cryostat. A different setup was used for recording the room-temperature PL spectra. It consisted of a 0.5-m grating monochromator and a PbS detector with lock-in techniques, for dispersion and detection purposes, respectively.

The compositions of the layers were determined using an energy dispersive spectrophotometer attached to an ISI SS-40 scanning electron microscope. GaSb, GaP, and InAs were used as the binary standards for Sb, Ga, In, and As, respectively. The quantitative analysis was carried out using Tracor Northern Computer. The MICROQ program with ZAF correction was used to analyze the x-ray spectra.

III. RESULTS AND DISCUSSION

A. Growth Results

GaSb and $Ga_{1-x}In_xAs_ySb_{1-y}$ layers of different compositions corresponding to the room-temperature PL peak wavelength range of 1.7–2.32 μm were grown by the LPEE technique. $Ga_{1-x}In_xAs_ySb_{1-y}$ layers of compositions corresponding to room-temperature PL peak wavelengths around 1.8, 1.99, and 2.2 μm have been labeled as α, β, and γ samples, respectively. The quaternary α and β layers were grown at 580 °C, as better compositional homogeneity is expected due to the reduction in the As distribution coefficient[7] at higher temperatures. However, for the growth of γ composition, catastrophic dissolution of the substrate occurred at this temperature due to the unstable melt. Hence the growth temperature was lowered to 530 °C. The liquidus compositions of the different melts used were reported earlier.[11] The growth parameters together with the results of lattice mismatch and the layer composition, where available, are given in Table I. The growth rate exhibited a linear dependence with the current density,[11] which is indicative of the dominance of the electrotransport mechanism in the growth process. The typical values of the growth rates as reported earlier[11] are 0.8 μm/min at a current density of 10 A/cm^2. Layers in the thickness range of 1–10 μm have been grown by this technique. The layers used for the PL measurements were 2–4 μm thick.

X-ray-diffraction studies of the grown layers indicated that epitaxial layer–GaSb substrate mismatch, $\Delta a/a$, never exceeded 0.17%. The full width half maxima (FWHM) of the epilayers were in the range of 20–67 arc sec. The good quality of the crystalline epilayers becomes evident when this is compared to the half-width of the 25–30 arc sec normally seen on the substrate itself. For α and β layers smooth and shiny surfaces were obtained with ease under both lattice-matched and lattice-mismatched conditions. This indicates that lattice matching is not critical for obtaining specular surfaces for compositions close to the GaSb corner of the phase diagram. For γ layers, the surface morphology was comparatively inferior, in general exhibiting a cloudy appearance. However, the exact dependence of the surface morphology on the lattice mismatch was not examined in detail.

B. Near band-edge PL spectra at 4.5 K

Figure 2 illustrates the 4.5-K PL spectra of LPEE-grown GaSb and $Ga_{1-x}In_xAs_ySb_{1-y}$ epilayers. The PL

TABLE I. Summary of growth conditions and characterization results. An asterisk indicates that the lattice mismatch was determined by high-resolution x-ray diffraction.

Sample No.	Growth temp. (°C)	Current density (A/cm^2)	Thickness (μm)	λ_{pl} (μm)	Eg (eV)	ΔEg (meV)	$\Delta a/a$ (%)	FWHM (arc sec)	x	y
GS-5	580	1.4	6.5	1.70	0.729	32				
GS-8				1.70	0.729	43			0.00	0.00
GS-29				1.71	0.729	37	0.00	24	0.00	0.00
*G*3α3				1.77	0.700	41		30		
αT-05	580	6.2		1.79	0.693	42	0.00	67		
αT-11	581	6.0		1.79	0.693	35	0.01	32	0.027	0.014
αT-02	580	8.2		1.81	0.685	37	−0.07	27		
α-23	581	10.4		1.81	0.685	39	0.00	31	0.028	0.016
αT-14	581	6.5		1.82	0.681	44	0.04	30		
α-21	581	9.9	5.5	1.84	0.674	35	0.04	20		
β-8				1.95	0.636	28				
β-9				1.96	0.633	32	0.048 *		0.088	0.056
β-120	574			1.96	0.633	35	0.001	30	0.098	0.058
βT-22	585	9.8	7.3	1.97	0.629	37	<0.050 *	42		
βT-27	572	7.5	3.7	1.99	0.623	35	−0.042	27	0.066	0.078
β-121	574			1.99	0.623	23	−0.083	40		
β-18	573	6.8	5.4	2.00	0.620	33	0.06	46		
γ-11	534	11.4	2.9	2.25	0.551		0.00 *	55		
γT-31	535	11.3	0.7	2.25	0.551	48	0.00	22	0.170	0.140
γT-47	532	18.7	3.7	2.26	0.549	37	−0.164 *	61	0.173	0.157
γT-46	535	14.4	4.0	2.27	0.546	37	−0.099 *	28	0.199	0.160
γT-44	535	8.9	3.7	2.27	0.546	45	0.083 *	66	0.191	0.164
γ-12	534	11.8	6.6	2.28	0.544	37	0.079 *	65	0.208	0.165
γ-14	533	11.7	3.7	2.30	0.539	41				
δAF-7	529	10.0	5.6	2.32	0.534	46			0.195	0.154

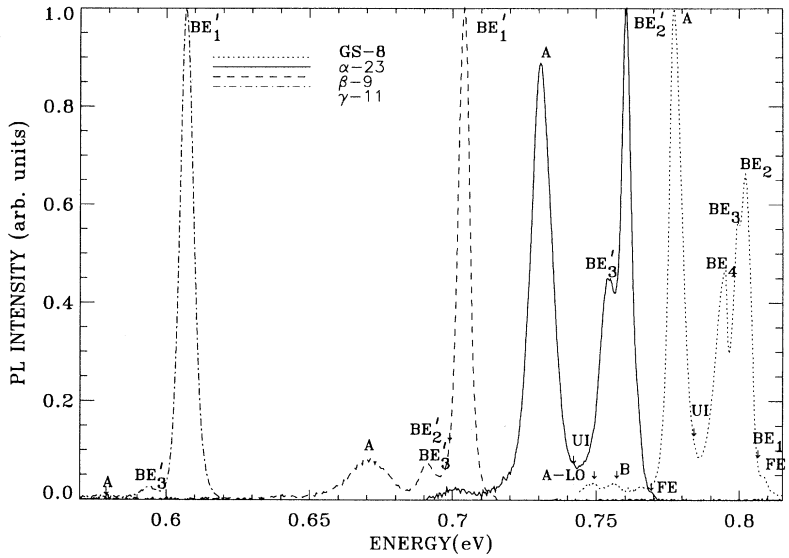

FIG. 2. Low-temperature (4.5 K) PL spectra of GaSb and $Ga_{1-x}In_xAs_ySb_{1-y}$ of three different compositions.

emission intensity of the spectra has been normalized with respect to the dominant peak present in each of the samples. A quantitative fit to the PL spectra, using the sum of Gaussian line shapes, has been utilized to accurately determine the peak positions and the spectral widths.

As shown in Fig. 2, in GaSb (sample GS-8) we observe four emission peaks labeled as BE_1, BE_2, BE_3, and BE_4 at 805.4, 802.2, 799.1, and 795.8 meV, respectively near the band edge. These peaks have been associated with the radiative decay of excitons bound to neutral acceptors. The origin of these acceptors is not definitely known though some have been conjectured as due to native defects. In addition, a weak transition associated with free excitons (FE) is also observed at 808.5 meV which attests to the high quality of the LPEE-grown layers. Amongst the bound exciton transitions, BE_2 is found to be the strongest and BE_1 appears to be hidden by the more pronounced emission peak BE_2, BE_3, and BE_4 also appear to be fairly strong.

The band-acceptor or donor-acceptor transition (A) at 777.5 meV is the dominant peak. In GaSb the donor levels are shallow ($\sim 2-3$ meV) due to the small effective mass of the electron, which makes it difficult to distinguish between free-to-bound and donor-to-acceptor recombination processes. A broad band at the lower energy can be resolved to consist of impurity-related transitions (B) and a phonon replica of A (A-LO). In addition to most of the peaks reported in the literature in LPE-grown GaSb, an additional unidentified peak (UI) at 784.6 meV observed in MBE (Ref. 35) and OMVPE (Ref. 36) grown layers, is also seen.

The PL spectra of the quaternary layers exhibit features similar to those described for GaSb. PL spectral characteristics of the quaternary layers are summarized in Table II. Free-exciton transition is seen only in the α-23 sample, as a weak band centered at 765.0 meV on the high-energy side of the spectrum. This is seen in both GaSb and α-23 layers only under the highest excitation level used. The highest-energy transition line identified as BE_2' at 760.5 meV becomes strong. In addition, we observe transitions at 754.3, 742.2, 730.6, and 702.2 meV which are labeled as BE_3', UI, A, and A-LO, respectively. The transitions BE_2' and BE_3' are relatively sharp and are

TABLE II. Low-temperature PL characteristics of LPEE-grown $Ga_{1-x}In_xAs_ySb_{1-y}$ layers. Relative intensity is denoted by Relat. Int.

	α-23			β-9			γ-11		
Identity	Energy (meV)	FWHM (meV)	Relat. Int.	Energy (meV)	FWHM (meV)	Relat. Int.	Energy (meV)	FWHM (meV)	Relat. Int.
FE	765.0	4.7							
BE_1'				703.8	5.0	1.0	607.1	5.5	1.0
BE_2'	760.5	4.1	1.00	697.9	5.2	0.04			
BE_3'	754.3	7.6	0.48	691.1	6.7	0.07	594.1	7.6	0.02
UI	742.2	14.0	0.07						
A	730.6	8.5	0.97	670.9	15.7	0.08	578.1		0.002
A-LO	702.2	8.8	0.03	640.2					

only 4.5 and 10.7 meV lower in energy than the free-exciton line. We suggest that these two transitions are associated with the decay of excitons bound to two different neutral acceptors whose identities are not known at this time. As in GaSb the transitions A and A-LO are associated with the band-acceptor recombination and its optical phonon replica, respectively, and transition A is the most intense. The energy band gap of this sample is obtained by adding the free-exciton binding energy (~ 1.1 meV) to the free-exciton transition energy (765.0 meV).

In sample β-9, which has an alloy composition corresponding to a lower band gap, we observe at least five transitions at 703.8, 697.9, 691.1, 670.9, and 640.2 meV labeled as BE_1', BE_2', BE_3' A, and A-LO, respectively. We do not see any evidence of the free-exciton transition for the range of pumping power studied in this work, and therefore cannot accurately determine the value of the energy band gap in this sample. We find that the linewidths of BE_1', BE_2' and BE_3' transitions observed in this sample are comparable to those of acceptor-bound excitons in GaSb and α-23 sample. We therefore suggest, as before, that these transitions are associated with the radiative decay of excitons bound to neutral acceptors. Additional support for this assignment is also provided by the excitation and temperature-dependent behavior of these transitions as described in an upcoming part of this paper. Thus if we assume that BE_1' is an acceptor-bound exciton transition, we can estimate the band gap of this sample by adding approximately 4 meV (namely, the sum of the exciton dissociation energy and FE binding energy) to the transition energy of BE_1', namely, 703.8 meV. This gives us a band gap of about 708 meV. The A transition, associated with the radiative recombination of a free electron with a bound hole of an acceptor is rather weak in this sample, whereas in GaSb and in α-23 it is the most intense transition. It is not clear why this transition is so weak whereas an acceptor-bound exciton transition BE_1' is so strong. From the value of the band gap and the transition energy of A we determine the binding energy of the acceptor to be 38 meV. This value compares quite well with those determined in GaSb (34 meV) and the α-23 sample (35 meV).

A broad line shifted by ~ 30 meV from the A peak towards lower energy appears, as in the other two samples. We label this structure the LO phonon replica of A (A-LO), as this energy corresponds to the optical phonon energy reported in GaSb.[37] In GaSb, α-23, and β-9 samples, the ratios of the intensity of the A peak and A-LO peak are in the range 32–40 and remain invariant within experimental error with excitation laser power intensity and decrease with increase in temperature. This trend conforms to the expected behavior of the phonon sideband further strengthening the assignment of this peak. However, $Ga_{1-x}In_xAs_ySb_{1-y}$ alloy have an unusual band structure and the peak designated as A-LO could be related to it. Even though this transition is proposed to be a phonon replica of A, this identification is by no means definite.

In sample γ-11, which has an alloy composition corresponding to even a lower band gap, we observe three transitions at 607.1, 594.1, and 578.1 meV labeled as BE_1', BE_3', and A, respectively. Again, we do not see a free excitonic transition. As in the case of sample β-9, we associate BE_1' and BE_3' with radiative recombination of excitons bound to two different neutral acceptors and estimate the band gap of this sample by adding about 4 meV to the transition energy of BE_1', namely, 607.1 meV. This leads to a band gap of about 611 meV. The transition A is very weak and could be detected only under high sensitivity. As before, we suggest that this transition is associated with radiative recombination of a free electron with a bound hole. The binding energy of an acceptor obtained in this case is about 33 meV which compares rather well with values obtained in GaSb and other two alloy samples. It should be pointed out that our observation of a single strong peak in γ samples is consistent with the experimental observation[2,38] on the layers grown by nonequilibrium techniques (OMVPE and MBE) where only one strong peak is seen for layers with compositions closer to or inside the miscibility gap region.

C. Intensity dependence of the PL spectra

To further confirm the identity of the various peaks, the PL spectra were studied as a function of incident laser power intensity. The integrated intensity of the BE_2' transition as a function of incident intensity for α samples is depicted in Fig. 3. It exhibits a power dependence of $P^{1.40}$. The transitions identified as BE_3' in all the quaternary layers exhibit an identical power dependence of $P^{1.22}$, though only the intensity dependence of BE_3' in α samples is shown, suggesting that the BE_3' transitions in the different quaternary layers have similar origin. These values are somewhat higher than the power dependence of $P^{0.96}$ and $P^{1.14}$, respectively, reported in GaSb layers for similar transitions by Chidley *et al.*[36]

In Fig. 4 we display the variation of the integrated intensity of BE_1' transition in β-9 sample as a function of the incident power. This transition exhibits a power dependence of 2.1. Similar power dependence for this transition is also found in the other quaternary alloy γ-11. We have calculated the power dependence of the integrated intensity of transitions associated with the radiative recombination of excitons bound to neutral acceptors using the well-known rate equations. We find that this dependence varies from $P^{1.0}$ to $P^{2.0}$ depending upon the values of the various recombination parameters which are highly sample dependent. Thus our assignment of BE_1', BE_2', and BE_3' transitions in $Ga_{1-x}In_xAs_ySb_{1-y}$ alloys to acceptor-bound excitons is consistent with their behavior as a function of incident power.

With the decrease of incident laser intensity, the higher-energy transitions gradually collapse and only the free electron to acceptor transitions persist at low intensities. The variation of the luminescence intensity of the free electron to acceptor peak in the β-9 layer at 670.9 meV as a function of incident intensity is also shown in Fig. 4. The intensity variation is perfectly linear with a slope of 1.0 confirming the assignment of this peak. No saturation effects in any of the peaks were observed in the limited range of incident laser power used.

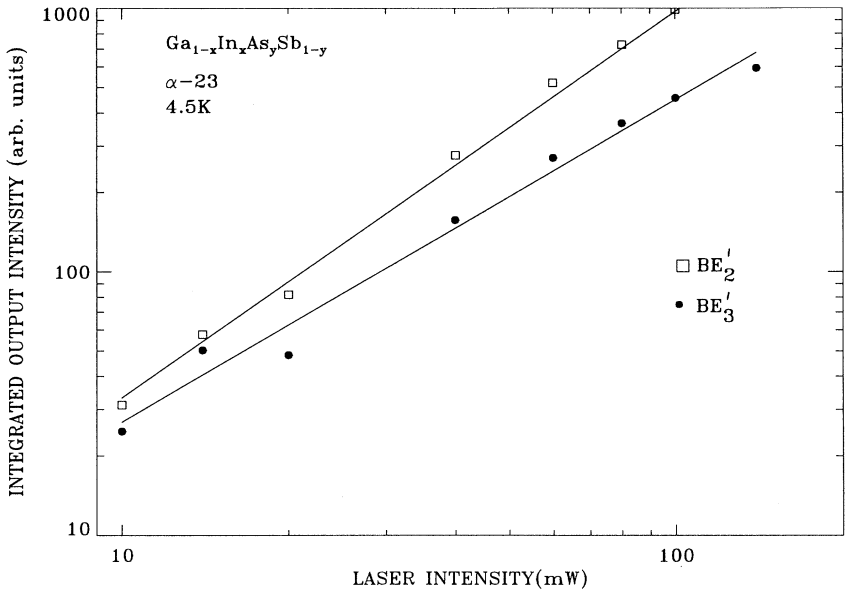

FIG. 3. Variation of PL-integrated intensity of the bound excitons as a function of the incident laser intensity in α layers.

D. Temperature dependence of the PL intensity

With increase in temperature, the overall integrated emission intensity of the quaternary PL spectra gradually decreases, indicating the presence of nonradiative mechanisms of decay with low activation energies. BE_2' in α layers shifts to higher energy by 0.57 meV with increasing temperature up to 30 K, and thereafter merges with the band-to-band transitions. The deeper bound exciton peak identified as BE_3' is rapidly quenched by 35–40 K with no significant shift in the position.

To determine the activation energies of the bound excitons, the low-temperature integrated intensity-dependent data for BE_3' were fitted as shown in Fig. 5, using the three-level Boltzmann distribution developed by Bimberg, Sondergeld, and Grobe,[39]

$$I_T/I_0 = 1/\{1 + C_1 \exp(-\Delta E_1/kT) + C_2 \exp(-\Delta E_2/kT)\}\ , \quad (1)$$

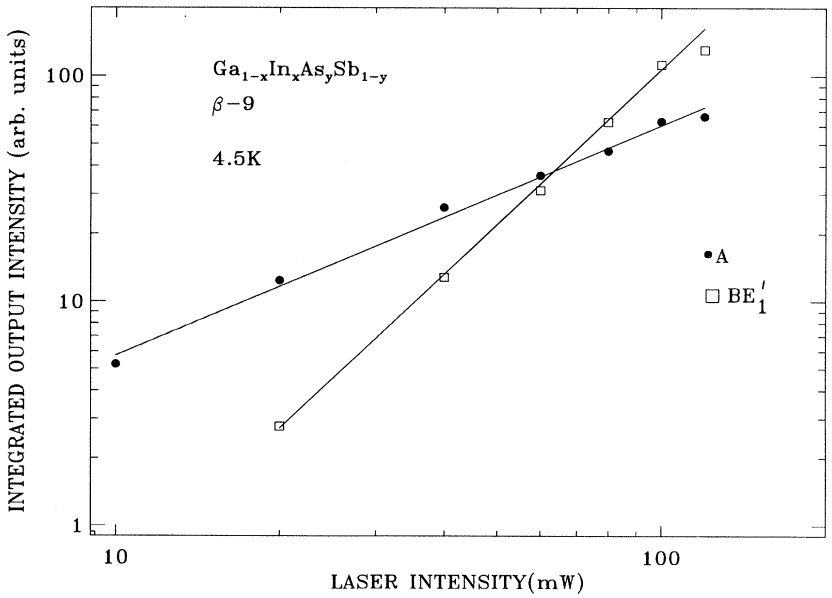

FIG. 4. PL-integrated intensity dependence of band-to-band transitions and band-to-acceptor transitions in β layers on the incident laser intensity.

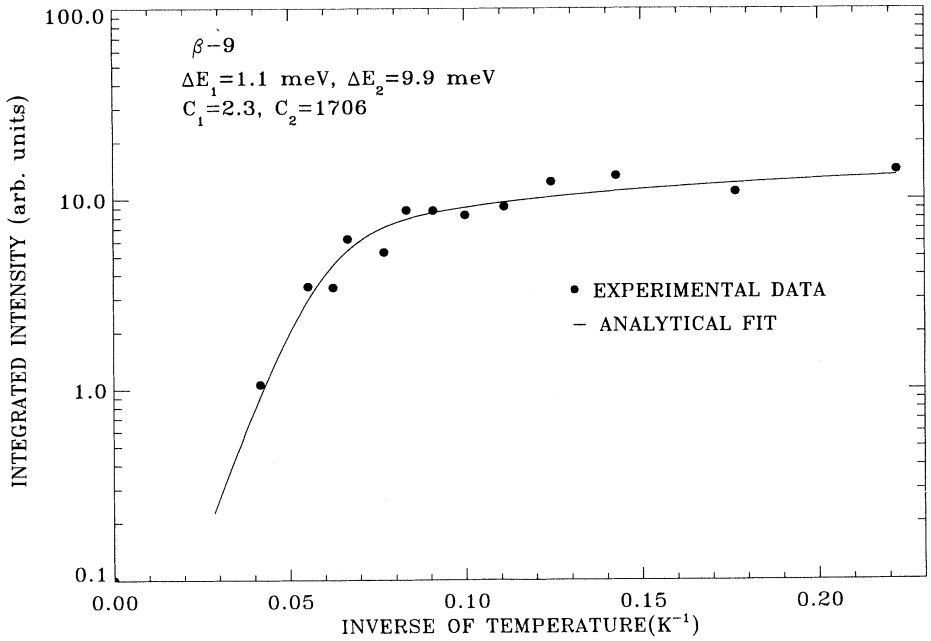

FIG. 5. Theoretical fit to the temperature dependence of integrated intensity of the deeper bound exciton transition (BE_3') at low temperatures. The values of C_1, C_2, and the binding energies are in excellent agreement with the results of GaSb (Ref. 33).

where I_T/I_0 represents the normalized integrated intensity at 4.5 K, ΔE_1 and ΔE_2 represent the effective-mass donor binding energy and dissociation energy of the bound exciton, respectively, and C_1 and C_2 are constants and are functions of the density of states. The values of ΔE_1 and ΔE_2 were found to be in the range 1.1–1.3 meV and 8.9–11 meV, respectively, in excellent agreement with the corresponding values reported in GaSb layers.[33] The binding energy of the second level ($\frac{4}{3}$ of the thermal activation energy) is in the range of 11.8–14.6 meV, which is also close to the values estimated from the PL peak positions. The intensity of BE_1' transitions as a function of temperature could not be fitted with a reasonable set of values for ΔE_1 and ΔE_2. The reason for this behavior is not clear at this time.

Integrated intensity of the band-to-acceptor transition also decreases with increase in temperature. However, it persists up to a temperature of 100–140 K. In α layers

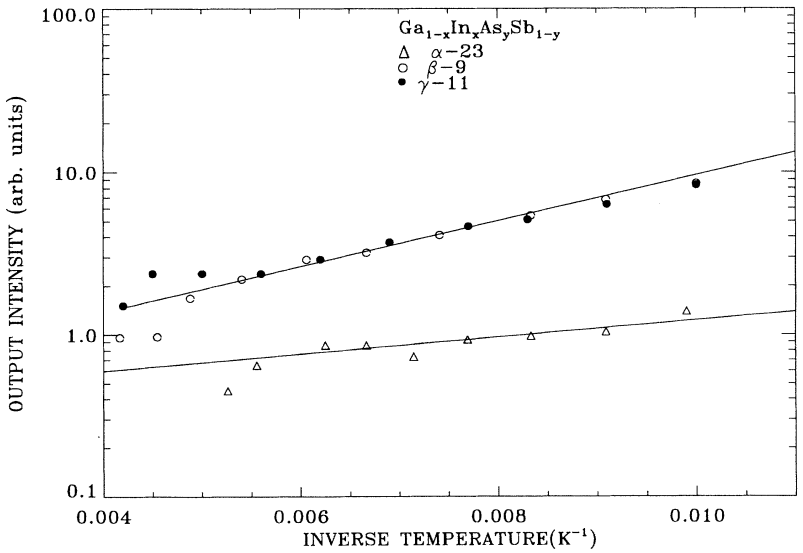

FIG. 6. Thermal quenching behavior of band-to-band PL emission for temperatures beyond 80 K. The intensity of the γ layers were scaled up so that they can be plotted on the same graph.

the A peak shifts to higher energy by 0.43 meV with a rise in temperature up to 35 K before it follows the band-gap variation. This may be caused by the shift in the quasi Fermi level to higher values in the conduction band, and consequent recombination of the free electrons above the Fermi level with the holes localized in the acceptor states.

The band-to-band transitions are the only recombination processes above 80 K in all the quaternary layers. With the rise in temperature the integrated intensity of the band-to-band transition decreases. The activation energy for this thermal quenching process has been determined using the configuration coordinate model, where the competing nonradiative recombination process can be described by the expression

$$I = I_0 \exp(E_a/kT) \tag{2}$$

where I and E_a represent the PL emission intensity and quenching activation energy, respectively. The semilogarithmic plot of intensity versus reciprocal temperature is linear as illustrated in Fig. 6 exhibiting an activation energy of 14 meV in α layer and 28 meV in β and γ layers. The fact that these energies do not correspond to the band-gap energy is indicative of the presence of various nonradiative centers in the quaternary layers. Such nonradiative recombination processes would degrade the performance of devices which have these alloys as active layers. They lead to a low value of T_0 for instance, which represents a characteristic temperature that relates to the laser threshold current density, J_{th} in the laser diode. The temperature dependence of J_{th} is described by

$$J_{\text{th}} = J_0 \exp(T/T_0) \tag{3}$$

where J_0 is the threshold current density at $T=0$ K. Phenomenologically, temperature dependence of the PL process could be expressed in terms of T_0 as

$$I \propto \exp(-T/T_0) . \tag{4}$$

The straight-line fit of the integrated intensity with temperature as shown in Fig. 7 yields the value of T_0 to be 225 K for the α sample and $\sim$90 K for β and γ samples, respectively. The latter result is in good agreement with the reported value of 80 K in $Ga_{1-x}In_xAs_ySb_{1-y}/Al_{1-x}Ga_xAs_ySb_{1-y}$ cw lasers;[40] the emission wavelength at 190 K being 2.1 μm, close to that of γ sample.

E. Line-shape analysis

For GaSb and quaternary samples all the PL peaks could be well fitted by the sum of the Gaussian line distributions at low temperatures. With a rise in temperature the PL spectra become increasingly asymmetrical, and the asymmetry sets in around the 25–35 K range indicating the dominance of the band-to-band transitions. The PL spectral shape of the band-to-band transition is analyzed[41] using

$$I(\omega) \propto (\hbar\omega - E_g)^{1/2} \exp[-(\hbar\omega - E_g)/kT] , \quad \text{for } \hbar\omega > E_m \tag{5}$$

$$\propto \exp[(\hbar\omega - E_g)/\epsilon] , \quad \text{for } \hbar\omega < E_m , \tag{6}$$

where ϵ is the tail-state parameter and E_m is the PL peak energy. The slope of the high-energy side of the spectrum is dependent on the sample temperature, while the lower-energy side of the spectrum is determined by the shape of the band edges. Figure 8 shows the experimental spectra and analytical fit for the γ layer at 80 K. A

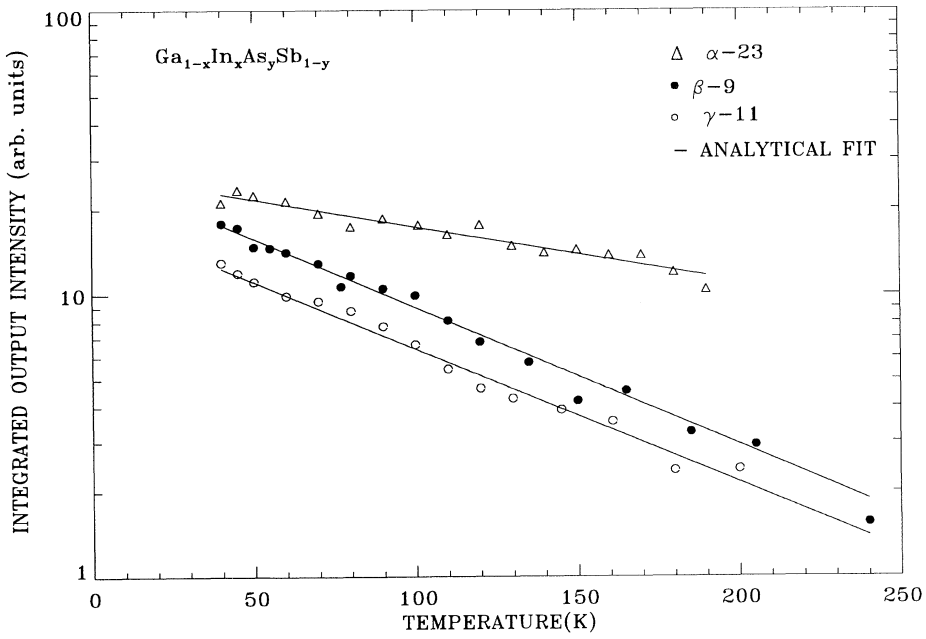

FIG. 7. Semilogarithmic plot of integrated intensity of band-to-band transitions as a function of temperature for all three different compositions of $Ga_{1-x}In_xAs_ySb_{1-y}$.

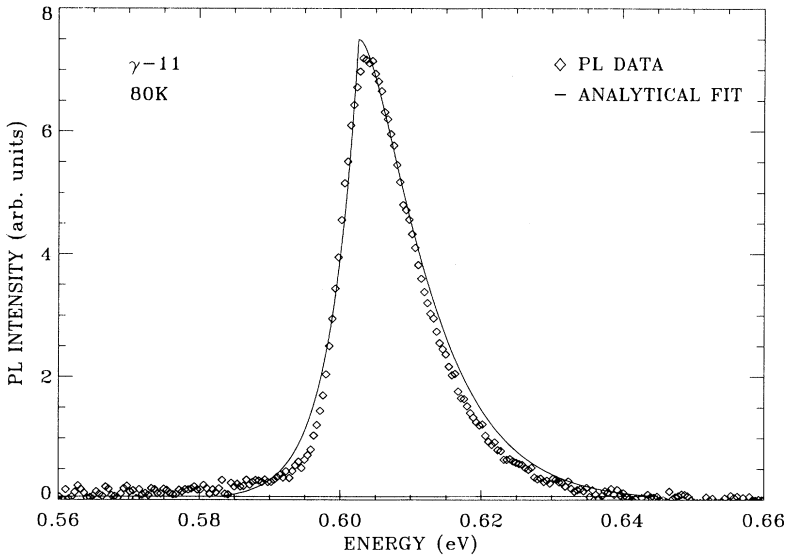

FIG. 8. Analytical fit to the PL spectra of γ layers at 80 K. The band-tail state parameter $\epsilon = 3$ meV was used to get the best fit to the lower-energy side of the spectrum.

similar fit has been obtained for all the quaternary layers in the temperature range 30–300 K with ϵ ranging from 3 to 10 meV. A similar behavior has also been observed in another quaternary $Ga_{1-x}In_xAs_yP_{1-y}/InP$ system.[42] This suggests that localized states formed either due to impurities or compositional grading contributes to the recombination processes. At higher temperatures, the emission spectra are narrower than the analytical spectra on the high-energy side, as self-absorption due to higher photon energy within the epilayer has not been taken into account. The value of E_g determined from this analysis was found to be $kT/2$ less than the PL peak energy indicative of k-conservation nature of the recombination processes.

The value of FWHM of the bound excitons for the quaternary alloys were in the range of 4–7 meV at 4 K. These are the smallest linewidths reported for $Ga_{1-x}In_xAs_ySb_{1-y}$ on GaSb so far. Variation of the FWHM of the band-to-band transitions the layers with temperature was also examined. Though there is a considerable scatter in the data, the experimental values for FWHM appear to increase linearly with temperature for all the layers, as shown in Fig. 9. The slopes of the lines are 1.0 k, 0.8 k, and 1.2 k for the three layers α, β, and γ,

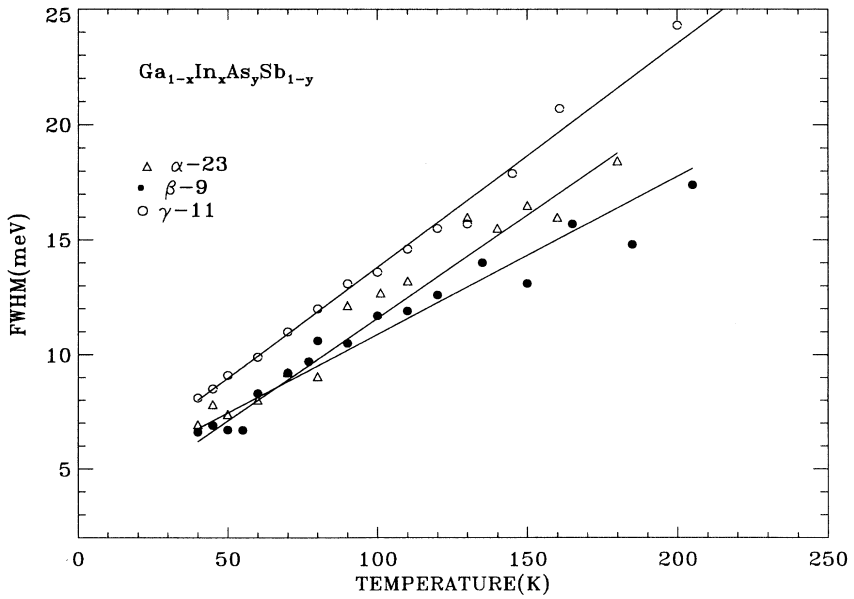

FIG. 9. Temperature dependence of the FWHM of band-to-band transitions in $Ga_{1-x}In_xAs_ySb_{1-y}$ layers.

respectively, and are much smaller than the analytical value of (1.8–2) k for an intrinsic band-to-band transition computed from Eq. (5). A similar discrepancy between the experimental and the computed half-width dependence on temperature has also been noticed in the $Ga_{1-x}In_xAs_yP_{1-y}$ system[43,44] and, as mentioned earlier, is commonly attributed to the overestimation of the spectral width by the van Roosbroeck–Shockley relation [Eq. (5)]. However, the narrow linewidths observed in our quaternary samples indicate the high quality of the crystalline layers.

And, finally, we would like to point out that our proposed assignment of the near band-edge emission peaks, BE_1', BE_2', and BE_3' to radiative recombination of excitons bound to different neutral acceptors in $Ga_{1-x}In_xAs_ySb_{1-y}$ layers is based on their relatively narrow widths and their behavior as a function of incident laser power and temperature. However, there are a few aspects of our data which are rather intriguing. For instance, in sample α-23, both the bound exciton peak BE_2' and electron-to-acceptor transition A are quite strong. However, in samples β-9 and γ-11, the intensities of peaks A are much smaller than those of BE_1'. If the BE_1' transition is due to exciton bound to neutral acceptors, as we have suggested, then the electron to the same acceptor transition should have been quite strong. Also in GaSb and sample α-23, we see several bound exciton peaks, but only one strong electron-to-acceptor transition. It is clear that more work needs to be done, especially in higher purity samples, to understand these features and to gain a better understanding of the nature of the acceptors.

IV. CONCLUSIONS

Good optical-device-quality layers of GaSb and $Ga_{1-x}In_xAs_ySb_{1-y}$ have been grown by LPEE technique as evidenced by the narrow spectral width of x-ray-diffraction and PL spectra. A systematic trend in the low-temperature PL spectra is observed with the change in the composition of $Ga_{1-x}In_xAs_ySb_{1-y}$. The optical activation energy of the acceptor is about 35 meV and its phonon replica is shifted by about 30 meV towards the lower energy, consistent with the reported values in GaSb. The dissociation energies of the bound excitons in quaternary layers were also in good agreement with those in the binary layers. A good fit to the PL spectral line shape due to band-to-band transition was obtained using the simple model of van Roosbroeck–Shockley at higher energies and exponential band edge at lower energies. The PL transitions appear to be k conserved from the data presented.

ACKNOWLEDGMENTS

We wish to thank Lori Small for assisting in the computer simulation of a few of the graphs, Soon Lau from AT&T Bell Labs and Mike Caparo for x-ray-diffraction measurements and Gernot Pomrenke for helpful suggestions. This work was supported by AFOSR (Contract No. F49620-89-C-004) and U.S ARO (Grant No. DAAL03-89-G-0115). The work of S.H. was supported by the U.S. Air Force (Contract No. F33615-88-C-5423).

[1]M. J. Cherng, H. R. Jen, C. A. Larsen, G. B. Stringfellow, H. Lundt, and P. C. Taylor, J. Cryst. Growth **77**, 408 (1986).
[2]M. J. Cherng, G. B. Stringfellow, D. W. Kisker, A. K. Srivastava, and J. L. Zyskind, Appl. Phys. Lett. **48**, 419 (1986).
[3]T. H. Chiu, J. L. Zyskind, and W. T. Tsang, J. Electron. Mater. **16**, 57 (1987).
[4]W. T. Tsang, T. H. Chiu, D. W. Kisker, and J. A. Ditzenberger, Appl. Phys. Lett. **46**, 283 (1985).
[5]J. C. DeWinter, M. A. Pollack, A. K. Srivastava, and J. L. Zyskind, J. Electron. Mater. **14**, 729 (1985).
[6]A. Joullie, F. Jia Hua, F. Karouta, and H. Mani, J. Cryst. Growth **75**, 309 (1986).
[7]M. Astles, H. Hill, A. J. Williams, P. J. Wright, and M. L. Young, J. Electron. Mater. **15**, 41 (1986).
[8]R. Sankaran and G. A. Antypas, J. Cryst. Growth **36**, 198 (1976).
[9]E. R. Gertner, A. M. Andrews, L. O. Bubulac, D. T. Cheung, M. J. Ludowise, and R. A. Riedel, J. Electron. Mater. **8**, 545 (1979).
[10]N. Kobayashi and Y. Horikoshi, Jpn. J. Appl. Phys. **20**, 2253 (1981).
[11]Shanthi N. Iyer, Ali Abul-Fadl, Albert T. Macrander, Jonathan H. Lewis, Ward J. Collis, and James W. Sulhoff, in *Layer Structures: Heteroepitaxy, Superlattices, Strain, and Metastability,* edited by B. W. Dodson, L. K. Schowalter, J. E. Cunningham, and F. H. Pollak, MRS Symposia Proceedings No. 160 (Materials Research Society, Pittsburgh, 1990), p. 445.
[12]A. Okamoto, J. Lagowski, and H. C. Gatos, J. Appl. Phys. **53**, 1706 (1982).
[13]Y. Imamura, L. Jastrzebski, and H. C. Gatos, J. Electrochem. Soc. **125**, 1560 (1978).
[14]J. J. Daniele and A. Lewis, J. Electron. Mater. **12**, 1015 (1983).
[15]J. J. Daniele and A. J. Hebling, J. Appl. Phys. **52**, 4325 (1981).
[16]M. Kumagawa, A. F. Witt, M. Lichtensteiger, and H. C. Gatos, J. Electrochem. Soc. **120**, 583 (1973).
[17]C. Takenaka, T. Kusunoki, and K. Nakajima, J. Cryst. Growth **114**, 293 (1991).
[18]Toshiharu Kawabata and Susumu Koike, Appl. Phys. Lett. **43**, 490 (1983).
[19]S. Iyer, E. K. Stefanakos, A. Abul-Fadl, and W. J. Collis, J. Cryst. Growth **67**, 337 (1984).
[20]A. Abul-Fadl, E. K. Stefanakos, and W. J. Collis, J. Electron. Mater. **11**, 559 (1982).
[21]K. Nakajima and S. Yamazaki, J. Cryst. Growth **74**, 39 (1986).
[22]S. Iyer, E. K. Stefanakos, A. Abul-Fadl, and W. J. Collis, J. Cryst. Growth **70**, 162 (1985).
[23]D. Effer and P. J. Etter, J. Phys. Chem. Solids **25**, 451 (1964).
[24]M. H. van Maaren, J. Phys. Chem. Solids **27**, 472 (1966).
[25]Y. J. Van Der Meulen, J. Phys. Chem. Solids **28**, 25 (1967).
[26]C. Anayama, T. Tanahashi, H. Kuwatsuka, S. Nishiyama, S. Isozumi, and K. Nakajima, Appl. Phys. Lett. **56**, 239 (1990).

[27]C. Benoit a la Guillaume and P. Lavallard, Phys. Rev. B **5**, 4900 (1972).
[28]A. S. Kyuregyan, I. K. Lazareva, V. M. Stuchebnikov, and A. E. Yunovich, Fiz. Tekh. Poluprovodn. **6**, 242 (1972) [Sov. Phys. Semicond. **6**, 208 (1972)].
[29]A. A. Kastal'skii, T. Risbaev, I. M. Fishman, and Yu. G. Shreter, Fiz. Tekh. Poluprovodn. **5**, 1596 (1972) [Sov. Phys. Semicond. **5**, 1391 (1972)].
[30]E. J. Johnson and H. Y. Fan, Phys. Rev. **139**, A1991 (1965).
[31]W. Jakowetz, W. Ruhle, K. Breuninger, and M. Pilkuhn, Phys. Status Solidi A **12**, 169 (1972).
[32]W. Ruhle and D. Bimberg, Phys. Rev. B **12**, 2382 (1975).
[33]W. Ruhle, W. Jakowetz, C. Wolk, R. Linnebach, and M. Pilkuhn, Phys. Status Solidi B **73**, 255 (1976).
[34]Fred H. Pollak and R. L. Aggarwal. Phys. Rev. B **4**, 432 (1971).
[35]M. Lee, D. J. Nicholas, K. E. Singer, and B. Hamilton, J. Appl. Phys. **59**, 2895 (1986).
[36]E. T. R. Chidley, S. K. Haywood, A. B. Henriques, N. J. Mason, R. J. Nicholas, and P. J. Walker, Semicond. Sci. Technol. **6**, 45 (1991).
[37]C. Pickering, J. Electron. Mater. **15**, 51 (1986).
[38]S. J. Eglash and H. K. Choi, in *Gallium Arsenide and Related Compounds, 1991,* edited by G. B. Stringfellow (IOP, London, 1992), p. 487.
[39]D. Bimberg, M. Sondergeld, and E. Grobe, Phys. Rev. B **4**, 3451 (1971).
[40]C. Caneau, A. K. Srivastava, J. L. Zyskind, J. W. Sulhoff, A. G. Dentai, and M. A. Pollack, Appl. Phys. Lett. **49**, 55 (1986).
[41]E. W. Williams and H. B. Bebb, in *Semiconductors and Semimetals,* edited by R. K. Willardson and A. C. Beer (Academic, New York, 1972), Vol. 4, Chap. 4.
[42]Ernst O. Gobel, in *GaInAsP Alloy Semiconductors,* edited by T. P. Pearsall (Wiley Interscience, New York, 1982), p. 320.
[43]T. P. Pearsall, L. Eaves, and J. C. Portal, J. Appl. Phys. **54**, 1037 (1983).
[44]H. Kyuragi, A. Suzuki, S. Matsumura, and H. Matsunami, Appl. Phys. Lett. **37**, 723 (1980).